Resonant Waves in the Gap between Two Advancing Barges

Liang Li [a], Zhiming Yuan [b,a], Chunyan Ji [b,*], Yan Gao [a]

[a] *Department of Naval Architecture, Ocean and Marine Engineering, University of Strathclyde, 100 Montrose Street, Glasgow, G4 0LZ, UK*

[b] *School of Naval Architecture and Ocean Engineering, Jiangsu University of Science and Technology, Zhenjiang, 212003, China*

Abstract

The gap resonance between two advancing rectangular barges in side-by-side arrangement is investigated using a 3-D Rankine source method. A modified Sommerfeld radiation condition accounting for Doppler shift is applied for the low forward speed problem when the scattered waves could propagate ahead of the barges. Numerical studies are conducted to investigate various factors which will influence the wave resonance in the narrow gap with particular attention paid on the forward speed effect and its coupling effects with gap width and draft. It is found that in the absence of forward speed, the trapped water surface oscillates like a flexible plate and the wave flow within the gap behaves like a standing wave. When the two barges are travelling ahead, the resonant wave patterns within the gap are reshaped. Additionally, the resonant frequencies shift to lower value and are compressed within a narrow range. Gap resonances are reduced by the augment of gap width. The effect of draft is shown to be associated with resonant modes. Draft effect becomes less pronounced at higher order resonant modes. Furthermore, both gap width and draft effects on gap resonance are found to be independent from forward speed.

Keywords: Gap resonance; forward speed; hydrodynamic interaction; Rankine source method; ship-to-ship problem

1. Introduction

Due to the increasing exploration of oil and gas in deep and ultra-deep waters, more side-by-side operations have been adopted in the marine industry. Zhao et al. [1] investigated the hydrodynamic interaction between a FLNG and a LNG carried in side-by-side configuration. Zhao et al. [2] predicted the hydrodynamic performance of a FLNG system during offloading operation. Traditional offloading operation involves ship-to-ship interaction in the absence of forward speed. But recent years have seen an increasing number of lightering operations, due to the restrictions during cargo vessel calling at ports or navigating in shallow waters. In a typical lightering operation, the cargo vessel and service vessel are moored to each other and sail at a low speed. In this specific circumstance, the gap resonance can be quite complicated with the addition of forward speed effect. Therefore, a reliable analysis methodology should be developed to predict the wave resonance behaviour during a lightering operation.

Potential flow theory has been widely applied in the study of gap wave resonance between two side-by-side floating bodies. Under the assumption of infinite water depth and infinite body length, Molin [3] derived a quasi-analytical approximation of natural modes of the inner free surfaces within a rectangular moonpool. Gap resonance between two adjacent ships in close proximity is very similar to moonpool resonance. The only fundamental difference is that, for the gap resonance problem (open-ended moonpool problem), a Dirichlet condition rather than the Neumann condition should be imposed to the open ends [4]. By applying the same approach, Molin et al. [5] expanded the analytical approximation of moonpool natural modes to gap resonance between two rectangular boxes. Sun et al. [6] studied the first and second order resonant waves between two adjacent barges. Influence of gap width was examined. Zhao et al. [7] investigated the first and higher harmonic components of gap response. Transient wave groups were used to avoid the wave reflection. It was found that the viscous damping has a linear form.

A shortcoming of the application of potential flow theory is the over-estimation of the gap resonance. Molin et al. [8] presented experimental evidence that the discrepancies between measured and predicted wave elevations were mostly due to the flow separation.

In order to analyse floaters with different corner radius, Moradi et al. [9] took the roundness factor into consideration by modifying the incident wave frequency. One of the popular solutions to the flow separation problem is the introduction of an artificial damping zone imposed on the water free surface. Yao and Dong [10] added an artificial damping surface and successfully overcame the over-estimation in their investigation of the gap resonance between two barges. An alternative approach is the application of computational fluid dynamics (CFD) technique, which can fully simulate the flow separation at sharp corners. Moradi et al. [11] examined the effect of water depth on gap resonance of two side-by-side rectangular boxes in a 2D numerical wave flume.

Generally, the study of gap resonance assumes that the two floating bodies have no forward speed, while investigations on forward speed problem are still inadequate. Fredriksen et al. [12] investigated resonant piston-mode resonance in a moonpool at low incoming current speed with both experimental and numerical methods. They found that the current speed had a slightly decreasing effect on the moonpool piston-mode. Lataire et al. [13] investigated the hydrodynamic forces acting on the ships during lightering operations in calm water. The mathematical model of lightering manoeuvres for both ships involved was derived. A typical challenge in forward speed problem is the satisfaction of radiation condition for outgoing waves, especially at low frequencies. This is because the waves generated ahead of a ship reflect from the outward computational boundary and smear the flow around the ship. One of the valid radiation conditions available for forward speed problem is the so-called upstream radiation condition [14], which truncates the free water surface at some upstream points and imposes different boundary conditions to the separated free water surface. Jensen et al. [15] proposed another approach by moving the panels on free water surface some distance downstream, namely the so-called panel shift technique. Both of the two approaches can achieve good agreement with experimental measurement at $\tau > 0.25$ ($\tau = u_0\omega_0/g$, u_0 is the ship speed, ω_0 is the wave frequency, and g is the gravity acceleration). However, the two approaches are based on the assumption that no scattered wave travel ahead of the ship so they are no longer valid for low forward speed problem at $\tau < 0.25$. Other categories of radiation condition applicable to low forward speed problem have been proposed and validated recently. Yasuda et al. [16] introduced Rayleigh's artificial friction in the boundary condition to suppress longer wave components in a computational region apart from the ship. Their simulation results showed that wave reflection from upstream boundary was very limited and good agreement with measured results was obtained as a result. Das and Cheung [17] proposed a modified Sommerfeld type radiation condition taking into account the Doppler shift effect of the scattered waves. Yuan et al. [18] expanded the radiation condition proposed by Das and Cheung [17] and investigated the hydrodynamic interaction between two ships travelling or stationary in shallow water. Their simulation results showed that this improved radiation condition has a better prediction capacity than upstream upwind condition in the case of low forward speed.

The primary objective of the present study is to investigate how forward speed influences the gap resonance between two barges in close proximity. Additionally, wave resonance behaviours in the case of different barge drafts and gap widths will be studied as well as their couplings with forward speed. A 3-D Rankine source method is applied to solve the boundary value problem and the radiation condition proposed in Ref [17] is used to dissipate the outgoing scattered waves.

2. Mathematical formulations

2.1. Boundary value problem

Assuming the flow field is ideal, linear potential flow theory is applied to model the wave resonance in the gap between two rectangular barges in lightering operation. The flow within the fluid domain is described by velocity potential $\Phi(\boldsymbol{r}, t)$ in which $\boldsymbol{r} = (x, y, z)$ denotes the position of the point concerned. $\Phi(\boldsymbol{r}, t)$ satisfies Laplace equation in the whole fluid domain. Consequently, the calculation of $\Phi(\boldsymbol{r}, t)$ is converted to boundary value problem.

The right-handed coordinate systems selected in the present study are shown in Fig. 1. O_0-$X_0Y_0Z_0$ is the global coordinate system. The centre O_0 is located on the mean sea surface and O_0Z_0 axis positive upward. The body-fixed coordinate systems *O-XYZ* is fixed to the two ships, with its origin located the centre of the gap and *OZ* axis positive upward. *dt* and *dl* represent the transverse and longitudinal distance between the two barges respectively. In the present research, dl = 0 m is used. The boundary value problem of each ship is addressed in the body-fixed coordinate system.

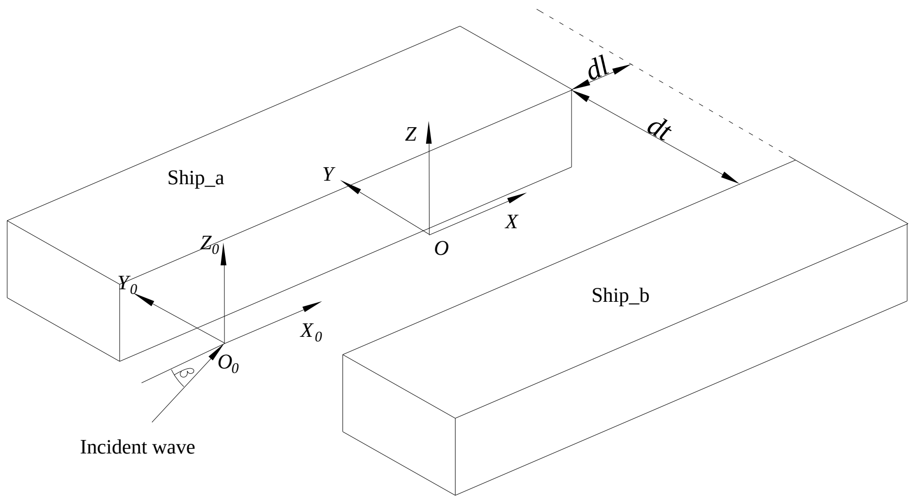

Fig. 1. Coordinate system.

In the present study, two rectangular barges are enforced to travel ahead together in head sea with the same forward speed and any oscillating motions are restricted. Consequently, the velocity potential within the fluid domain can be represented with Eq. (1) in the body-fixed coordinate system.

$$\Phi(\boldsymbol{r},t) = (\varphi_s(\boldsymbol{r}) - u_0 x) + \mathrm{Re}\sum_{j=0}^{1}\left[\eta_j\varphi_j(\boldsymbol{r})\cdot e^{-i\omega_e t}\right] \tag{1}$$

$\varphi_s(\boldsymbol{r})$ is the steady wave potential produced by the advancing movement of the ship. $\varphi_0(\boldsymbol{r})$ is the incident wave potential and η_0 is the wave amplitude. $\varphi_1(\boldsymbol{r})$ is the scattered wave potential with $\eta_1 = \eta_0$. ω_e is the encounter frequency, which is given by

$$\omega_e = \omega_0 - u_0\frac{\omega_0^2}{g}\cos\beta \tag{2}$$

where ω_0 is the incident wave frequency, β is the angle of wave heading (β = 180° corresponds to head sea).

The steady velocity potential is solved as

$$\begin{aligned}
&\nabla^2\varphi_s = 0, \textit{in the fluid domain} \\
&u_0^2\frac{\partial^2\varphi_s}{\partial x^2} + g\frac{\partial\varphi_s}{\partial z} = 0, \textit{on free water surface} \\
&\frac{\partial\varphi_s}{\partial n} = u_0 n_1, \textit{ on mean wetted surface of } \text{Ship_a} \\
&\frac{\partial\varphi_s}{\partial n} = u_0 n_1, \textit{ on mean wetted surface of } \text{Ship_b} \\
&\frac{\partial\varphi_s}{\partial n} = 0, \textit{on sea bed}
\end{aligned} \tag{3}$$

where $\boldsymbol{n} = (n_1, n_2, n_3)$ is the unit normal vector directed inward on body surface. $\boldsymbol{r} = (x, y, z)$ is the position vector. The generalised normal vectors n_j are defined as

$$n_j = \begin{cases} \boldsymbol{n}, \ j = 1,2,3 \\ \boldsymbol{r}\times\boldsymbol{n}, \ j = 4,5,6 \end{cases} \tag{4}$$

The scattered wave velocity potential $\varphi_1(\boldsymbol{r})$ is solved with Eq. (5).

$$\begin{aligned}
&\nabla^2\varphi_1 = 0, \textit{in the fluid domain} \\
&g\frac{\partial\varphi_1}{\partial z} - \omega_e^{\,2}\varphi_1 + 2i\omega_e u_0\frac{\partial\varphi_1}{\partial x} + u_0^{\,2}\frac{\partial^2\varphi_1}{\partial x^2} - i\omega_e u_0\frac{\partial^2\varphi_s}{\partial x^2}\varphi_1 - 2i\omega_e u_0\frac{\partial\varphi_s}{\partial x}\frac{\partial\varphi_1}{\partial x} \\
&= i\omega_e u_0\frac{\partial^2\varphi_s}{\partial x^2}\varphi_0 + 2i\omega_e u_0\frac{\partial\varphi_s}{\partial x}\frac{\partial\varphi_0}{\partial x}, \textit{ on free water surface} \\
&\frac{\partial\phi_1}{\partial\boldsymbol{n}} = -\frac{\partial\phi_0}{\partial\boldsymbol{n}}, \textit{ on mean wetted surface of } \text{Ship_a} \\
&\frac{\partial\phi_1}{\partial\boldsymbol{n}} = -\frac{\partial\phi_0}{\partial\boldsymbol{n}}, \textit{ on mean wetted surface of } \text{Ship_b} \\
&\frac{\partial\phi_1}{\partial z} = 0, \textit{ on sea bed}
\end{aligned} \tag{5}$$

The incident wave velocity potential $\varphi_0(\boldsymbol{r})$ is described with

$$\varphi_0(\boldsymbol{r}) = \frac{g}{i\omega_0}\cdot\frac{\cosh(kz+kH)}{\cosh(kH)}\cdot e^{-ik(x\cos\beta + y\sin\beta)} \tag{6}$$

The above boundary value problem will be completed with the addition of a suitable radiation condition imposed on the control surface and the velocity potential $\Phi(\boldsymbol{r}, t)$ is obtained subsequently.

The modified Sommerfeld radiation condition proposed by Das and Cheung [17] is used

$$\frac{\partial\varphi}{\partial\boldsymbol{n}} - ik_s\varphi\cos\theta = 0,\ \text{on } S_1$$
$$\nabla\varphi = 0,\ \text{on } S_2 \qquad (7)$$

where k_s is the local wave number. S_1 is a certain area in behind the two ships and S_2 is a certain area in front of the ships. Please refer to Das and Cheung [17] for more details of the development of this radiation condition.

2.2. Desingularied method

The classical Rankine source method requires distributing the singularity exactly on the boundary of the fluid domain. Nevertheless, a designularied method which raises the panels on the free water surface a short distance ∇z upward (see Fig. 2) is commonly used in a forward speed problem [19]. Meanwhile, the collocation points, where the boundary condition is satisfied, still stay exactly on the free water surface. Different values of the raised distance were reported by researchers. For instance, Zhang [20] used $\sqrt{S}$ as the raised distance (S is the area of the local mesh). In the present study, a raised distance ∇z=0.1L_j suggested by Kim et al. [21] is selected, where L_j is the diagonal length of panel j.

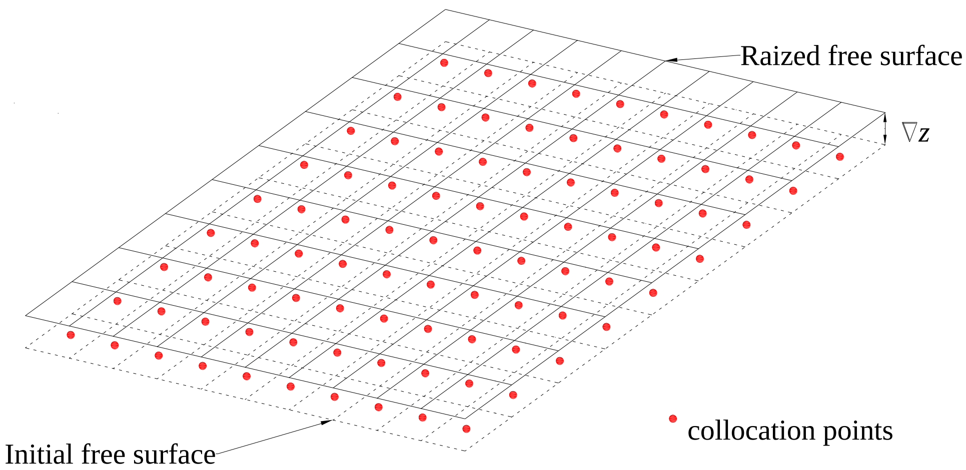

Fig. 2. Illustration of the raised mesh on the free surface.

The appearance of the second derivative of the potential in the free surface condition of diffraction potential requires special treatment. In theory, second derivative terms can be handled with analytical approach. However, it is found that the influence matrix tends to be ill-conditional when analytical representation is applied, which is likely to be caused by the large diagonal value of influence matrix. This kind of numerical phenomenon was firstly reported by Longuet-Higgins [22] in their time-domain study of steep surface waves. They found that the wave pattern developed a saw-toothed appearance in which the computed particle positions lay alternately above and below a smooth curve. Similar problem has been reported by Xu and Yue [23] as well. Similar problem may also happen in a frequency-domain analysis. Therefore, the present study applies a difference scheme rather than an analytical formula to represent the second derivative term. Common difference schemes are upwind difference scheme and central difference scheme. Generally, central difference scheme is more accurate while the stability of upwind difference is better. In addition, the application of upwind difference scheme enforces that the wave pattern mainly depends on upstream flow, which is consistent with physical observation. Due to this favorable property of upwind difference scheme, the second-order upwind difference scheme proposed by Bunnik [24] (see Fig. 3) is adopted to represent the second derivative of velocity potential:

$$\frac{\partial^2 \varphi}{\partial x^2}(\boldsymbol{r}_i) = \frac{1}{\Delta x_i^2}\left[\frac{1}{4}\varphi(\boldsymbol{r}_{i+4}) - 2\varphi(\boldsymbol{r}_{i+3}) + \frac{11}{2}\varphi(\boldsymbol{r}_{i+2}) - 6\varphi(\boldsymbol{r}_{i+1}) + \frac{9}{4}\varphi(\boldsymbol{r}_i)\right], i \le N-4 \quad (8)$$

where N is the number of panels on the straight line along the ship speed. For some panels, there are fewer than 5 panels in front. In that case, the following rule is used

$$\begin{aligned} &\frac{\partial^2 \varphi}{\partial x^2}(\boldsymbol{r}_i) = \frac{1}{\Delta x_i^2}\left[\varphi(\boldsymbol{r}_{i+1}) - 2\varphi(\boldsymbol{r}_i) + \varphi(\boldsymbol{r}_{i-1})\right], N-3 \le i \le N-1 \\ &\frac{\partial^2 \varphi}{\partial x^2}(\boldsymbol{r}_i) = \frac{\partial^2 \varphi}{\partial x^2}(\boldsymbol{r}_{i-1}), i = N \end{aligned} \quad (9)$$

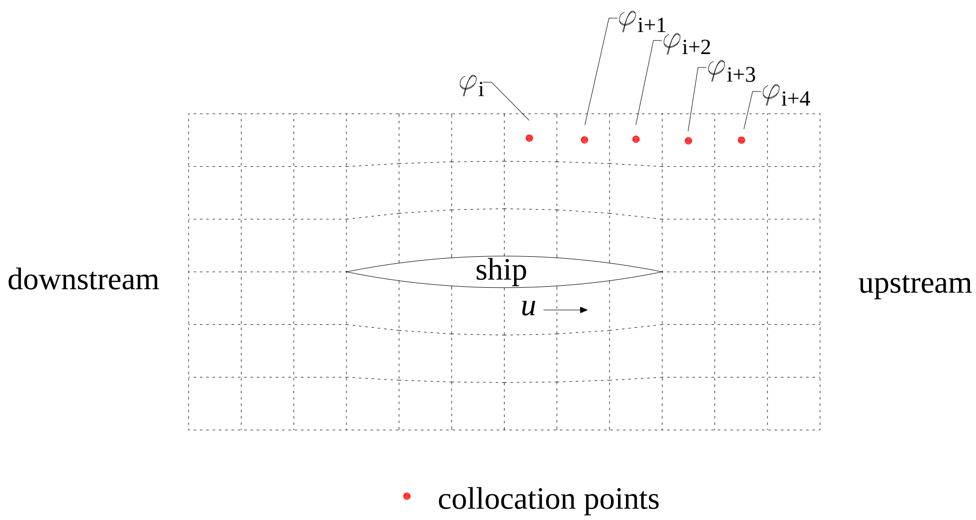

Fig. 3. Illustration of the second-order upwind difference scheme.

3. Validation

Model test research on side wall effect performed by Kashiwagi and Ohkusu [25] is quoted to validate the numerical program. Assuming that the two barges are identical to each other and advance with the same forward speed, the single ship problem in Fig. 4 (a) is identical to the ship-to-ship problem in Fig. 4 (b) as the Wall_1 in Fig. 4 (a) plays a role of mirror. In this way, the experimental data can be used to validate the numerical program.

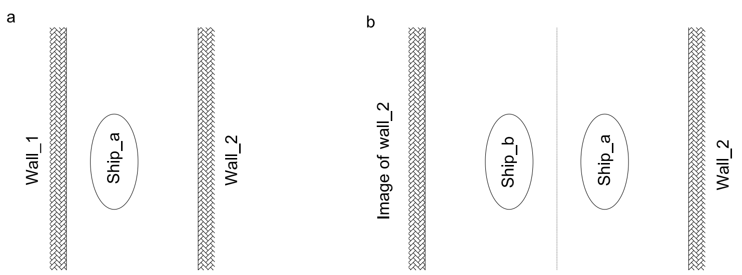

Fig. 4. Ship advancing in narrow waterway. (a) single ship problem; (b) two ships problem.

The ship model in the model test was a half-immersed prolate spheroid with length L = 2 m and breath B = 0.4 m. Water depth is set to 2.3 m. The spheroid is advancing at Froude number $F_n = 0.1$. The simulated and model test measured hydrodynamic forces of the spheroid are compared in Fig. 5. In general, the predicted hydrodynamic forces agree well with experimental data.

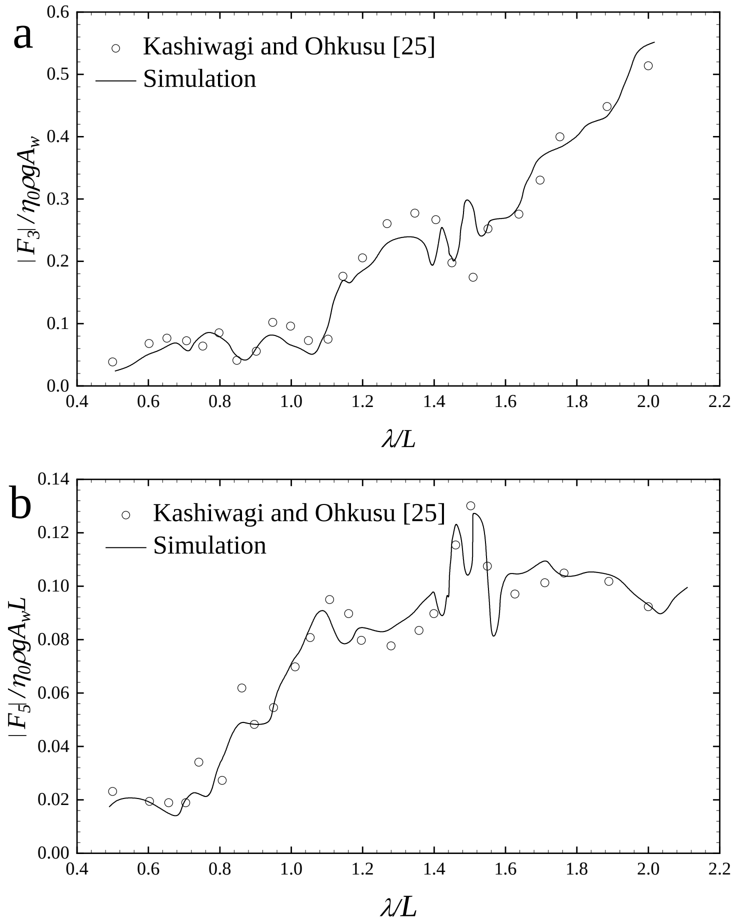

Fig. 5. Wave exciting forces of a half-immersed prolate spheroid. (a) heave wave exciting force; (b) pitch wave exciting moment. A_w is the water plane area and λ is the wave length.

4. Gap resonance between two advancing rectangular barges

In this section, the gap resonance between two side-by-side arranged rectangular barges during lightering operation will be investigated in terms of trapped wave elevation and transverse wave exciting force. Only head sea condition is considered in this study. The two barges are enforced to sail together with the same forward speed and any oscillating motions are restricted. Main dimensions of the barges are listed in Table 1. Water depth is set to 100 m. Simulation cases for a set of regular waves are performed to capture the gap resonance at a wide range of wave frequency. The wave amplitude is set to 1 m. Please also note that no extra damping is added in this study.

Table 1

Main dimensions of the rectangular barge

Item	Value
Length (*L*)	300 m
Breath (*B*)	75 m
Draft (*h*)	22 m
Displacement (*V*)	495,000 m^3
Gap width (*b*)	14.8 m

4.1. Forward speed effect

When two side-by-side arranged rectangular barges are travelling together with forward speed in head sea, the wave resonance in the gap is expected to exhibit unique characteristics compared with stationary condition. To figure out the forward speed effects on gap resonance, investigations will be conducted under different forward speed conditions.

Forward speed has been shown to modify the frequencies of resonant waves. Fig. 6 demonstrates the variation of resonant modes with forward speed. Table 2 summarizes the resonant frequencies at various resonant modes. When the two barges are stationary in wave, resonant wave elevation is observed around 0.532 rad/s, 0.584 rad/s and 0.64 rad/s. In the presence of forward speed, the resonant frequencies shift to lower values. In the body-fixed coordinate, the oscillating frequency of wave flow seen by the gap is larger than ω_0 if the two barges are travelling in head sea. It partly explains the shift of resonant frequencies in the presence of forward speed. It is also shown that the resonant frequencies are compressed within a narrow frequency range. Moreover, such effect becomes more prominent as the forward speed increases.

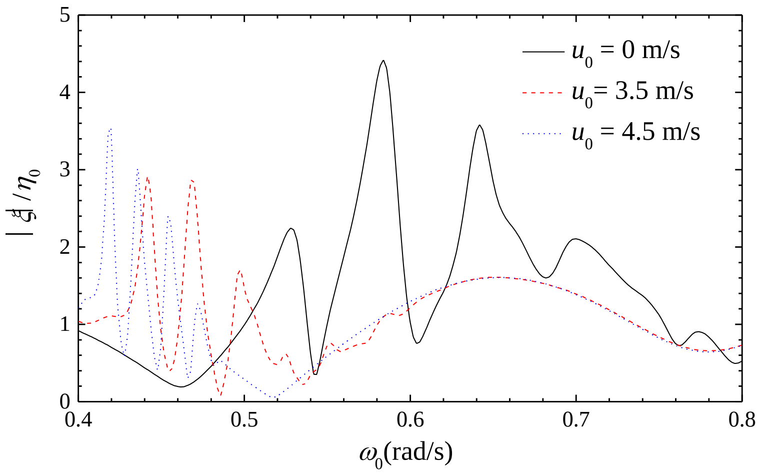

Fig. 6. Resonant frequencies of wave elevation at different forward speeds.

Table 2

Resonant frequencies of wave elevation at different forward speeds

	1st Mode	2nd Mode	3rd Mode
u = 0 m/s	0.532 rad/s	0.584 rad/s	0.64 rad/s
u = 3.5 m/s	0.442 rad/s	0.468 rad/s	0.496 rad/s
u = 4.5 m/s	0.418 rad/s	0.436 rad/s	0.454 rad/s

Fig. 7 demonstrates the amplitudes of resonant wave elevation along the central line of the gap (-150 m < X < 150 m, Y = 0 m) at different forward speeds. It is shown that wave patterns in the gap are closely associated with the resonant modes. In Fig. 7 (a), one single crest is observed around X = 0 m. The wave amplitude then decays gradually as it moves to the gap ends. At the 2nd mode, two crests appear at X = -90 m and X = 110 m, respectively. Nevertheless, a trough is observed around X = 0 m. At the 3rd mode, three crests are observed at X = -80 m, X = 0 m and X = 110 m whereas two troughs appear at X = -50 m and X = 60 m. Additionally, the maximum wave elevation drops at higher order of resonant modes. Fig. 8 presents a clearer demonstration of the wave surface oscillation at various resonant modes. The wave patterns of odd number modes are symmetric with respect to midship, while even number modes are antisymmetric. Analogous mode shapes can be expected occur at even higher modes. It appears that the water surface within the gap oscillates as a flexible plate. Similar phenomenon of waves between two barges in beam sea has been reported by Feng and Bai [26] as well. It can be also seen that forward speed effect reduces the amplitude of resonant waves. Although the nature of free surface oscillation seems not to be changed by the presence of forward speed according to Fig. 7 (b) and Fig. 7 (c), the wave patterns at resonant modes are reshaped. Fig. 9 compares the wave pattern of 3rd resonant mode when the two barges are travelling at u = 0 m/s and u_0 = 3.5 m/s, respectively. Compared the upper half part, no wave crest can be found at the upstream region of gap in the lower half part. It seems that the trapped free surface no longer oscillates like a flexible plate in the presence of forward speed.

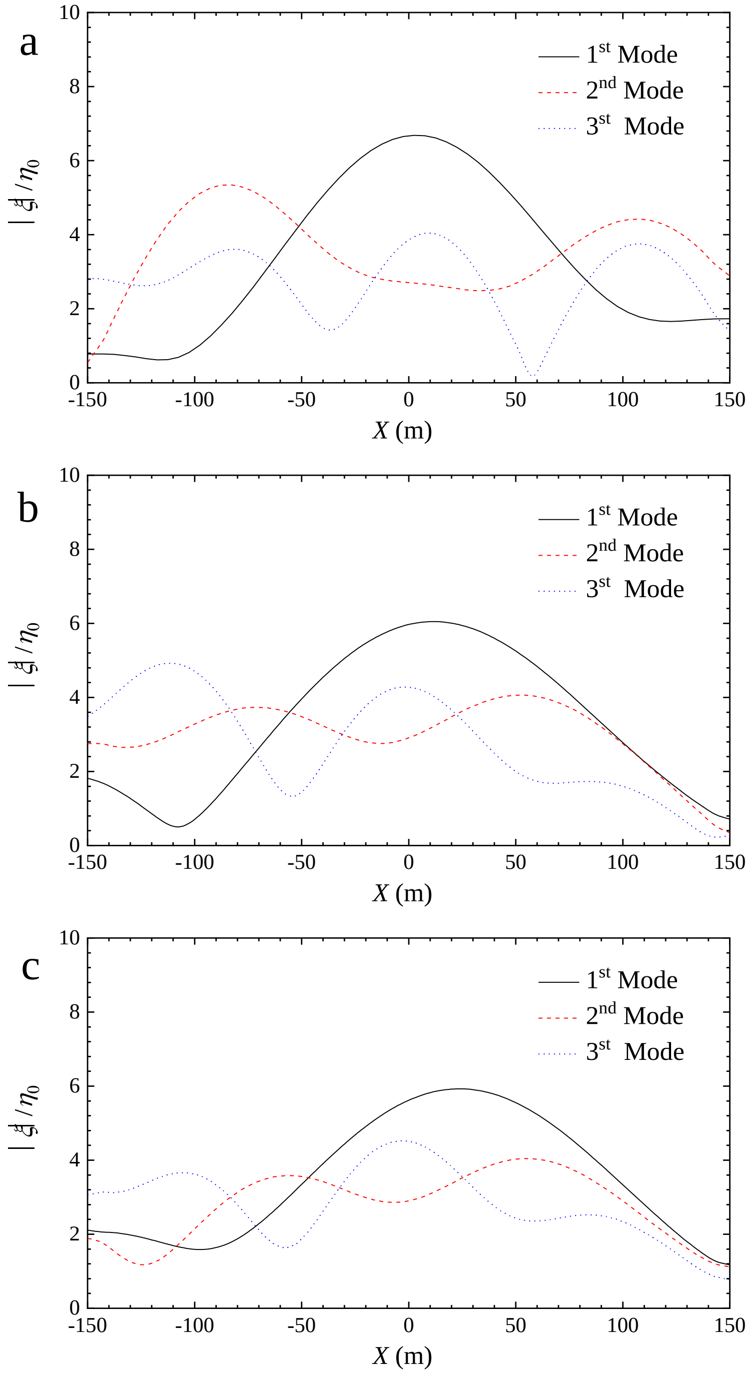

Fig. 7. Dimensionless wave elevation along the central line of gap at different forward

speeds. (a) u_0 = 0 m/s; (b) u_0 = 3.5 m/s; (c) u_0 = 4.5 m/s.

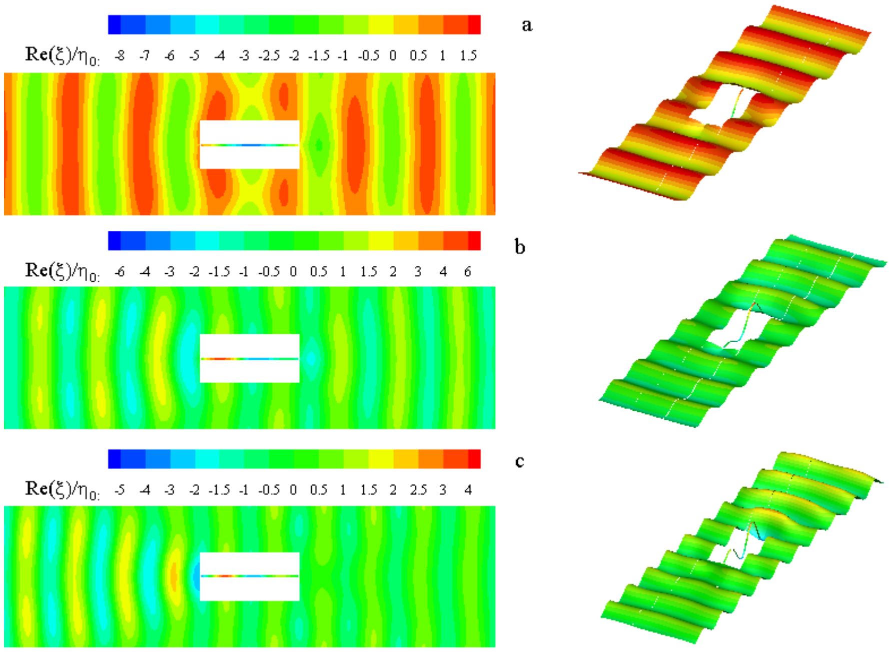

Fig. 8. Real part of wave patterns Re(ξ)/η_0 at various resonant modes, u_0 = 0 m/s (body-fixed coordinate system). (a) 1st mode; (b) 2nd mode; (3) 3rd mode.

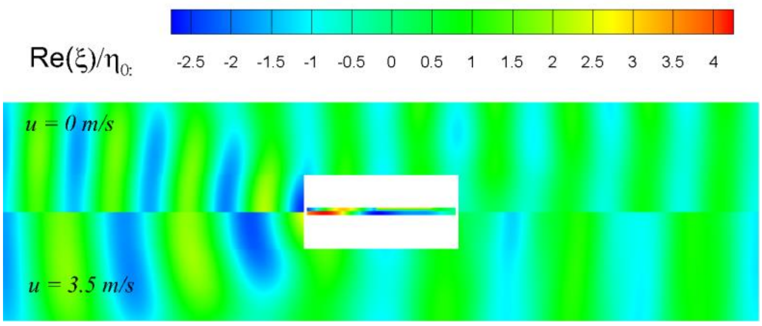

Fig. 9. Real part of wave patterns Re(ξ)/η_0 at 3rd resonant mode (body-fixed coordinate system).

To further investigate the gap water surface oscillation, Fig. 10 displays the instantaneous wave elevation along the central line at 3rd resonant mode. As shown in Fig. 10 (a), the wave flow within the gap behaves very like a standing wave, especially within the mid gap zone (-50 m < X < 50 m). Combing the wave surface profile at various time steps, it can be concluded that the wave surface indeed oscillates like a flexible plate. The standing wave pattern becomes less evident near the gap ends. This is because the physical boundary condition at gap ends is a Dirilect condition rather than a Neumann condition. It means that the fluid flow is free to move in and out of the envelop through the gap ends, resulting in fluid exchange and loss of wave energy trapped in the gap.

Consequently, the standing wave patterns around the gap ends are less obvious. When the two barges are travelling ahead, the standing wave behaviour becomes nearly invisible (see Fig. 10 (b)) and the oscillations of water surface are different from a flexible plate oscillation mode. As the barges are travelling ahead, the fluid exchange between the gap and outer field become more prominent. In this circumstance, the majority of wave energy used to be trapped within the envelope in stationary cases is now carried to the downstream. Please note that the wave energy also escapes from the bottom of the gap. Based on the CFD technology, Feng et al. [27] conducted a detailed investigation on the wave flow at the gap and they clearly showed the wave flow escaped from the bottom. However, the wave dissipation at the bottom is mainly due to the flow separation and shedding occurring at the square edge [28]. Since the linear potential flow theory is used in our model, it is out of the scope of the present study.

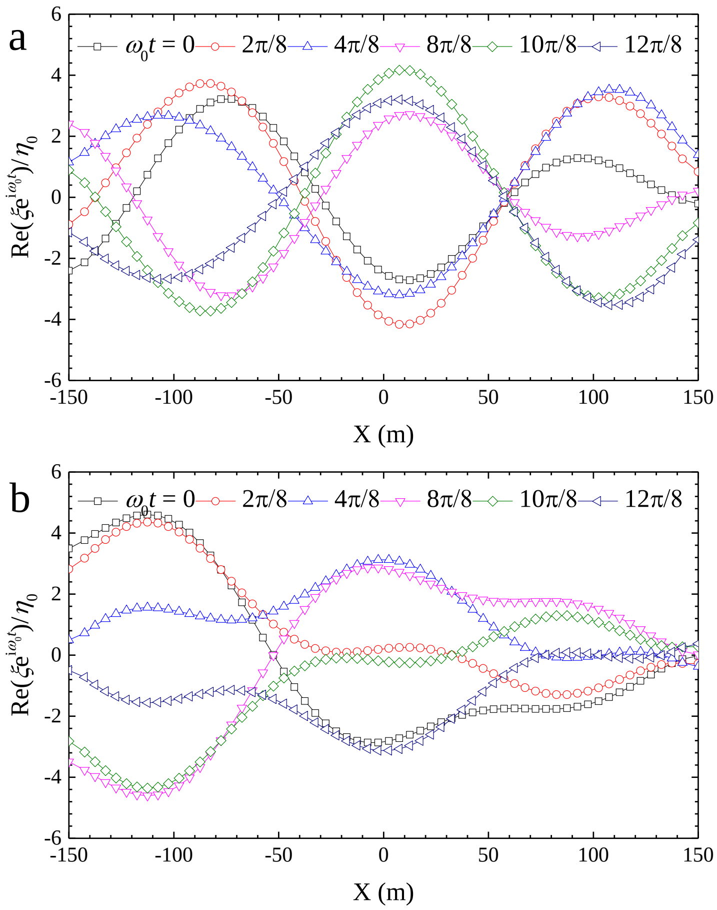

Fig. 10. Instantaneous wave elevation along the central line of gap at 3rd resonant mode. (a) u_0 = 0 m/s; (b) u_0 = 3.5 m/s.

In addition to wave elevation, the hydrodynamic wave force represents another aspect of gap resonances. The wave-induced transverse exciting forces on single barge are estimated at different forward speeds and the simulation results are presented in Fig. 11.

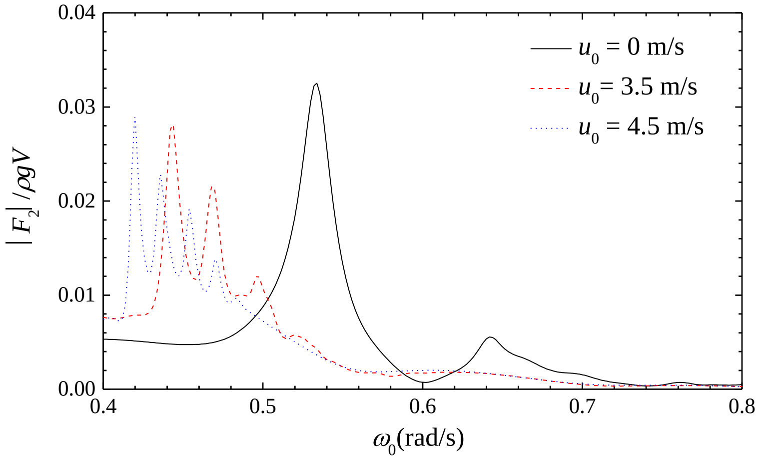

Fig. 11. Transverse wave exciting force on single barge at different forward speeds.

The resonant modes of transverse wave force vary with forward speed. When the two barges are stationary in waves, resonant wave exciting force is observed at around 0.534 rad/s and 0.642 rad/s, corresponding to the 1st and the 3rd resonant modes of wave elevation in Table 2. As the water wave pattern of even number resonant modes are antisymmetric with respect to midship (see Fig. 8 (b)), the transverse wave forces acting on the upstream half ship and downstream half ship just offset each other, resulting in a limited resultant transverse force. Therefore, the wave force is not excited at 2nd mode. In the presence of forward speed effect, extra resonant wave forces are excited and the resonant frequencies shift to lower value within a narrow frequency range. When the two barges are travelling ahead at u = 3.5 m/s, the resonant wave forces are excited at 0.444 rad/s, 0.468 rad/s and 0.496 rad/s, corresponding to the 1st, 2nd and 3rd resonant modes of wave elevation. Transverse wave force is excited at 2nd resonant mode because the wave patterns of even number order resonant modes are on longer antisymmetric with respect to midship. As a result, transverse wave force acting on the upstream half ship and downstream half ship would not offset each other. Such forward speed effect becomes more pronounced with the increase of forward speed. It can also be seen from Fig. 11 that the peak value of the 1st mode of resonance force decreases in the presence of forward speed. The decreased transverse force amplitude could reduce the risk of breaking mooring lines or hawsers during lighting operations.

According to the above discussions about gap resonance, forward speed plays a positive role in lightering operations. Forward speed contributes to the reduction of wave elevation and attracting or separating force by carrying wave energy to the downstream. Additionally, forward speed is able to modify the resonant frequencies of gap wave, indicating that the resonant responses can be avoided by adjusting the forward speed on the basis of local sea states. It will substantially reduce the chance of ships being subject to large amplitude impact loads and hence avoid potential accidents.

4.2. Gap width effect

The gap width between the two barges is varied from 9.8 m to 19.8 m with an increment 5 m to investigate the gap resonant responses at different gap widths. Additionally, gap resonances will be also investigated at zero and nonzero forward speed conditions to figure out whether the gap width effect would alter when coupled with forward speed effect.

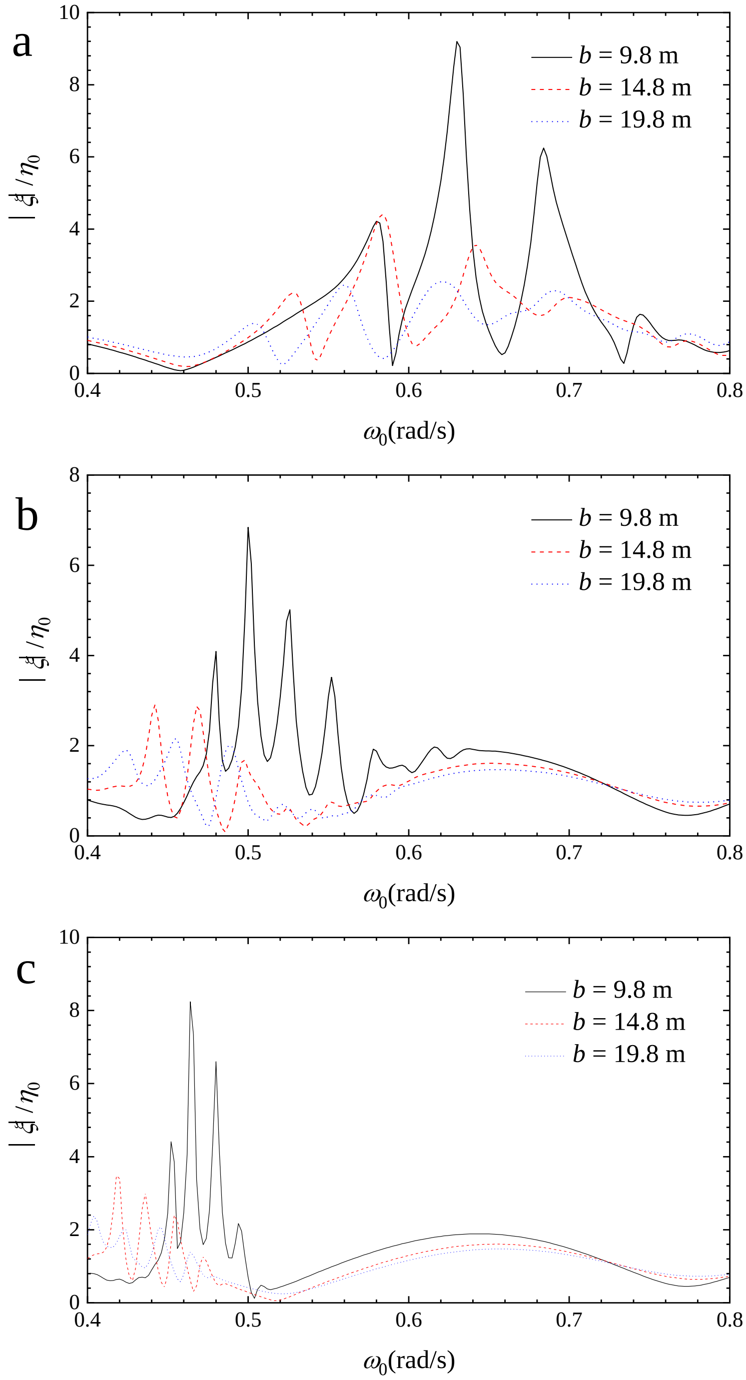

Fig. 12. Resonant frequencies of wave elevation at different gap widths. (a) $u_0 = 0$ m/s; (b) $u_0 = 3.5$ m/s; (c) $u_0 = 4.5$ m/s.

Fig. 12 compares the resonant frequencies at different gap widths. It is shown clearly that the resonant frequencies shift to lower values within a narrow range with the increase of gap width. This trend remains the same no matter the barges are stationary or moving ahead, manifesting that the gap width effect on the resonant frequencies is independent from forward speed effect. It also indicates if the sea state is known, the resonant frequencies can be avoided by adjusting the gap width between two barges.

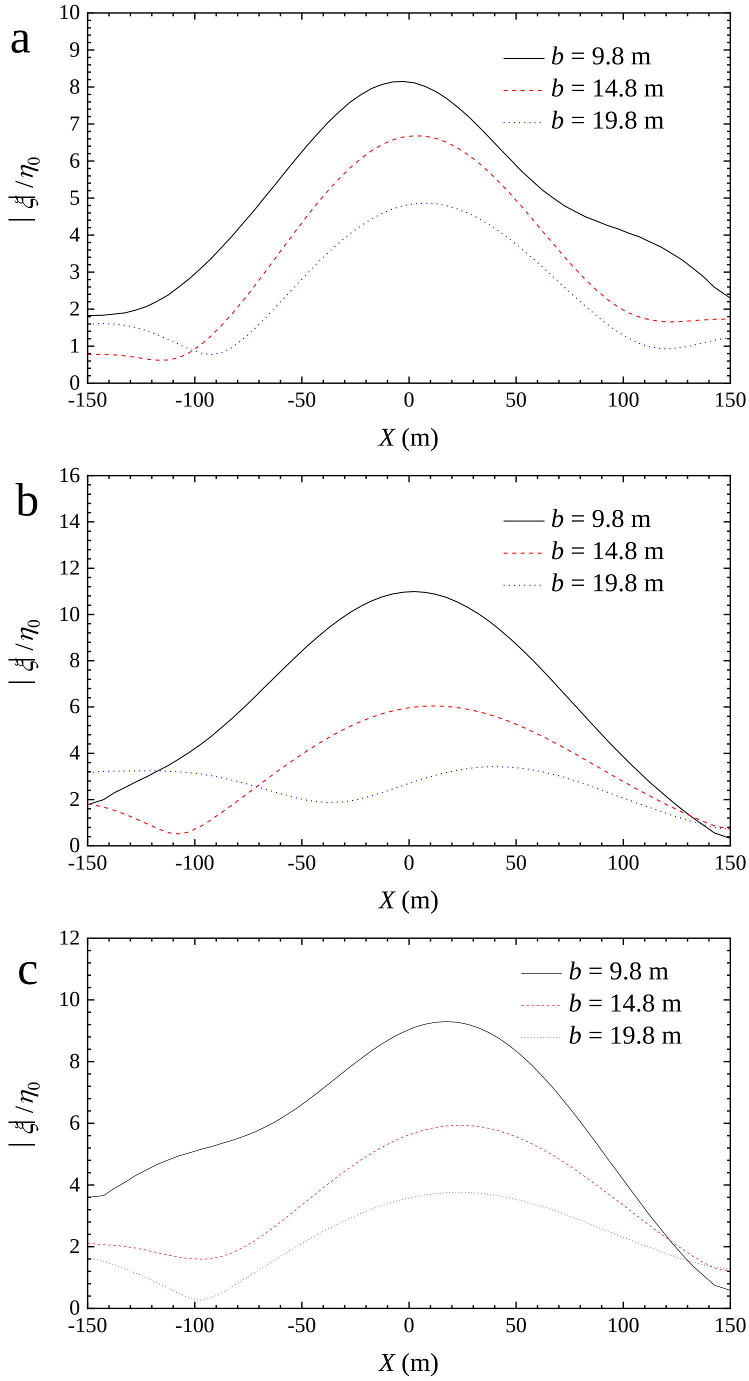

Fig. 13. Wave elevation along the central line of gap with different gap widths at 1st resonant mode; (a) u_0 = 0 m/s; (b) u_0 = 3.5 m/s; (c) u_0 = 4.5 m/s.

The wave elevation along the central line of gap at different gap widths is examined and the simulation results at 1st resonant mode are presented in Fig. 13. In general, increase of gap width contributes to the alleviation of gap resonance by reducing wave amplitudes within the gap, regardless of forward speed. The hydrodynamic interaction between the two barges becomes less pronounced with the increase of gap width and hence the gap resonance will reduce. Meanwhile, the change of gap width does not reshape the wave pattern at resonant mode. Fig. 14 compares the wave patterns within the gap with different widths (b = 14.8 m and b = 19.8 m, respectively) when the two barges are stationary in head sea. As shown, the wave patterns within the gap are very similar. A wave trough appears in the middle of gap and the wave elevation increases gradually as it moves to the gap ends.

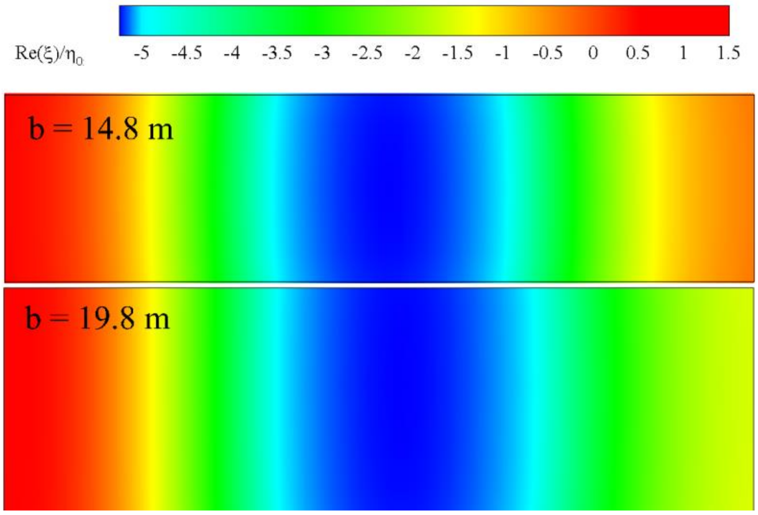

Fig. 14. Real part of wave patterns Re(ξ)/η_0 with different gap widths at 1st resonant mode, u_0 = 0 m/s (body-fixed coordinate system). Upper part represents case b = 14. 8 m; lower part represents case b =19.8 m.

The variation of transverse exciting forces with incident wave frequencies at different gap widths are shown in Fig. 15. The variation trend of wave forces follows a similar way as that of wave elevations. Both in stationary and travelling conditions, the resonant frequencies of transverse wave force shift to lower value within a narrow frequency range. Meanwhile, the amplitudes of wave force also drop as a result of less prominent hydrodynamic interaction.

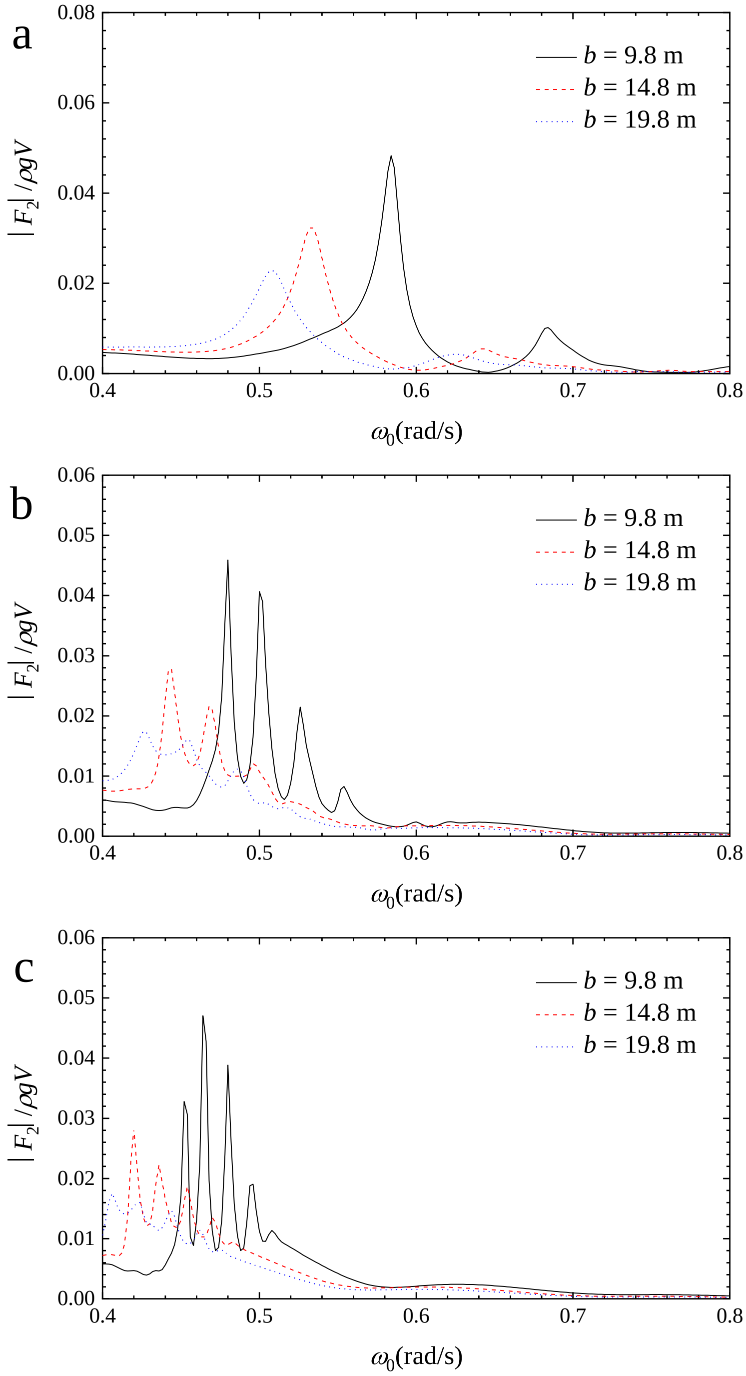

Fig. 15. Transverse wave exciting forces at different gap widths. (a) $u_0 = 0$ m/s; (b) $u_0 = 3.5$ m/s; (c) $u_0 = 4.5$ m/s.

4.3. Draft effect

Draft effect on the wave resonance is examined by adjusting the draft of the barges. The forward speed is also adjusted to investigate whether the draft effect will vary in the case of different forward speeds.

Fig. 16 presents the variation of wave elevation resonant frequencies with barge draft.

When the draft increases, the resonant frequencies shift to lower level. Moreover, this variation trend remains the same regardless of forward speed.

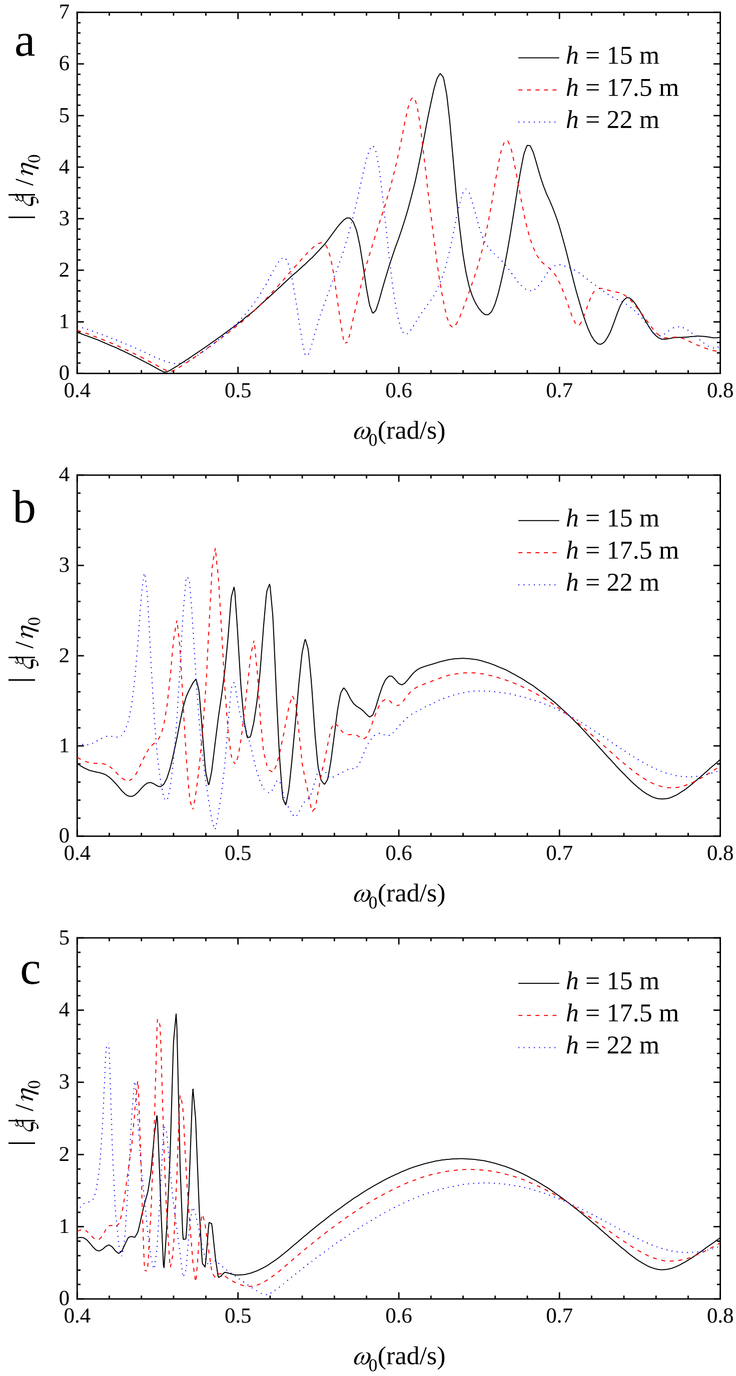

Fig. 16. Resonant frequencies of wave elevation at different barge drafts. (a) $u_0 = 0$ m/s; (b) $u_0 = 3.5$ m/s; (c) $u_0 = 4.5$ m/s.

The dependency of resonant wave elevation on barge draft is displayed in Fig. 17. In general, resonant wave elevation increases with barge draft reflecting that the gap resonance becomes more prominent. A deeper draft makes could trap more wave energy within the envelope. Consequently, the gap resonance becomes increasingly pronounced as a reflection of increasing amount of wave energy trapped. Once again, the variation of wave elevation with draft is independent from forward speed.

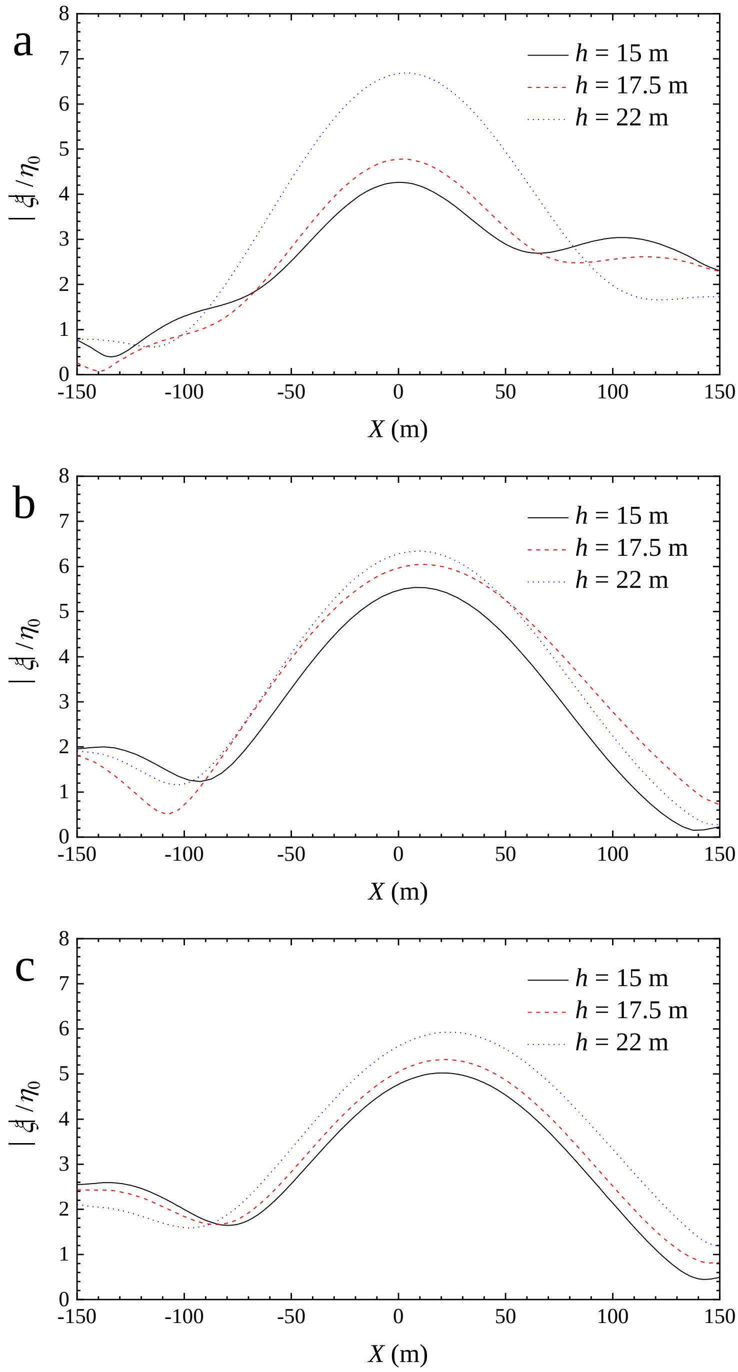

Fig. 17. Dimensionless wave elevation at different drafts. (a) 1st mode, u_0 = 0 m/s; (b) 1st mode, u_0 = 3.5 m/s; (c) u_0 = 4.5 m/s.

Fig. 18 displays the variation of transverse wave force as a function of incident wave frequency at different barge drafts. The transverse wave force varies with draft in a similar way like resonant wave elevation. The resonant frequencies of transverse wave force shift to lower value with the increase of draft. Meanwhile, there is also a positive correlation between transverse wave force and barge draft.

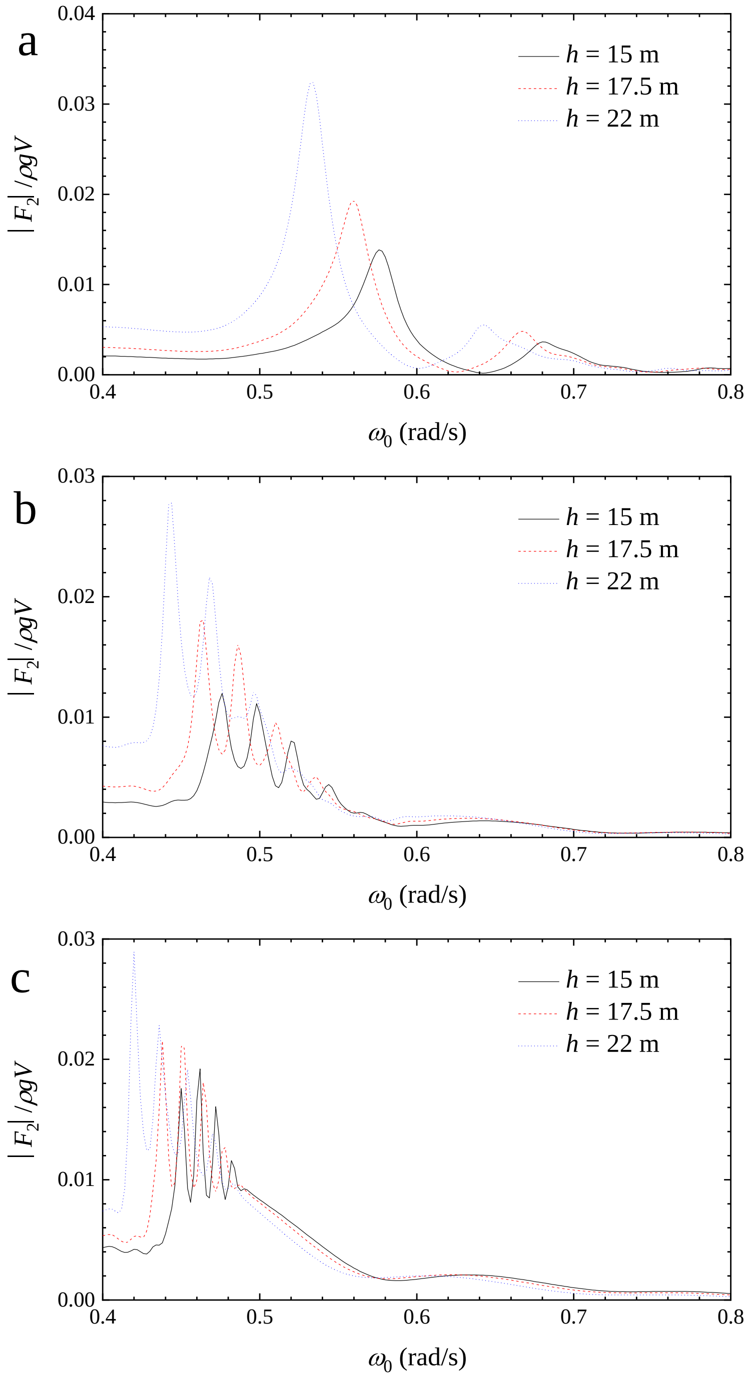

Fig. 18. Dimensionless wave force at different drafts. (a) u_0 = 0 m/s; (a) u_0 = 3.5 m/s; (a) u_0 = 4.5 m/s;

5. Conclusions

In the present study, a 3-D Rankine source method is applied to investigate the gap resonance between two travelling rectangular barges arranged side-by-side with concentration on the forward speed effects. The gap width effect and barge draft effect are also studied as well as their coupling effects with forward speed. A modified Sommerfeld radiation condition, accounting into the Doppler shift effect, is applied in this paper to manage the low forward speed problem ($\tau < 0.25$). The following conclusions have been drawn from the present study.

1. Forward speed effect reshaped the wave pattern within the gap and modified the resonant frequencies of gap resonance. Simulation results showed that the gap water surface no longer oscillated like a flexible plate in the presence of forward speed and the standing wave pattern became nearly invisible. In addition, the wave elevation was also reduced accounting into forward speed effect. Analysis manifested that forward speed accelerated the fluid exchange between the gap and outer fluid field, leading to the reduction of wave energy trapped within the envelop. Consequently, the gap resonance was reduced, in terms of wave amplitudes and wave exciting forces. In addition to the reduction of gap resonances, forward speed also shifted the resonant frequencies to lower values within a narrow frequency range. It indicated that the resonant responses can be avoided by adjusting forward speed in a lightering operation.
2. Augment of gap width contributed to the reduction of gap resonance as the hydrodynamic interaction between the two barges became less prominent. Meanwhile, the resonant frequencies shifted to lower values.
3. More wave energy gest trapped within the gap with a deeper draft, leading to the amplification of gap resonance responses. In addition, resonant frequencies shifted to lower values with the augment of draft.
4. The variation trend of gap resonance with respect to gap width and draft seems to be independent from the forward speed.

Acknowledgement

The third author is financially supported by National Natural Science Foundation of China [Grant No. 51622902 and 51579122].

References

[1] W.H. Zhao, J.M. Yang, Z.Q. Hu, Hydrodynamic Interaction between Flng Vessel and Lng Carrier in Side by Side Configuration, J Hydrodyn, 24 (2012) 648-657.

[2] W.H. Zhao, J.M. Yang, Z.Q. Hu, L.B. Tao, Prediction of hydrodynamic performance of an FLNG system in side-by-side offloading operation, J Fluid Struct, 46 (2014) 89-110.

[3] B. Molin, On the piston and sloshing modes in moonpools, Journal of Fluid Mechanics, 430 (2001) 27-50.

[4] J. Newman, P. Sclavounos, The computation of wave loads on large offshore structures, in: International Conference on the Behavior of Offshore Structures, Trondheim, 1988, pp. 605-622.

[5] B. Molin, F. Remy, O. Kimmoun, Y. Stassen, Experimental study of the wave propagation and decay in a channel through a rigid ice-sheet, Appl. Ocean Res, 24 (2002) 247-260.

[6] L. Sun, R.E. Taylor, P.H. Taylor, First-and second-order analysis of resonant waves between adjacent barges, J. Fluid Struct, 26 (2010) 954-978.

[7] W. Zhao, H.A. Wolgamot, P.H. Taylor, R. Eatock Taylor, Gap resonance and higher harmonics driven by focused transient wave groups, J. Fluid Mech, 812 (2017) 905-939.

[8] B. Molin, F. Remy, A. Camhi, A. Ledoux, Experimental and numerical study of the gap resonances in-between two rectangular barges, in: 13th congress of international maritime association of mediterranean, Instanbul, Turkey, 2009.

[9] N. Moradi, T.M. Zhou, L. Cheng, Effect of inlet configuration on wave resonance in the narrow gap of two fixed bodies in close proximity, Ocean Eng, 103 (2015) 88-102.

[10] C.B. Yao, W.C. Dong, Modeling of fluid resonance in-between two floating

structures in close proximity, J Zhejiang Univ-Sc A, 16 (2015) 987-1000.

[11] N. Moradi, T. Zhou, L. Cheng, Two-dimensional numerical study on the effect of water depth on resonance behaviour of the fluid trapped between two side-by-side bodies, Appl. Ocean Res, 58 (2016) 218-231.

[12] A.G. Fredriksen, T. Kristiansen, O.M. Faltinsen, Experimental and numerical investigation of wave resonance in moonpools at low forward speed, Appl. Ocean Res, 47 (2014) 28-46.

[13] E. Lataire, M. Vantorre, G. Delefortrie, M. Candries, Mathematical modelling of forces acting on ships during lightering operations, Ocean Eng, 55 (2012) 101-115.

[14] D.E. Nakos, P.D. Sclavounos, On steady and unsteady ship wave patterns, Journal of Fluid Mechanics, 215 (2006) 263.

[15] G. Jensen, H. Soding, Z. Mi, Rankine source methods for numerical solutions of the steady wave resistance problem, in: 16th Symposium on Naval Hydrodynamics, 1986, pp. 575-581.

[16] E. Yasuda, H. Iwashita, M. Kashiwagi, Improvement of Rankine Panel Method for Seakeeping Prediction of a Ship in Low Frequency Region, in: 35th International Conference on Ocean, Offshore and Arctic Engineering, American Society of Mechanical Engineers, Busan, South Korea, 2016, pp. OMAE2016-54163.

[17] S. Das, K.F. Cheung, Scattered waves and motions of marine vessels advancing in a seaway, Wave Motion, 49 (2012) 181-197.

[18] Z.-M. Yuan, A. Incecik, S. Dai, D. Alexander, C.-Y. Ji, X. Zhang, Hydrodynamic interactions between two ships travelling or stationary in shallow waters, Ocean Eng, 108 (2015) 620-635.

[19] X.S. Zhang, P. Bandyk, R.F. Beck, Time-Domain Simulations of Radiation and Diffraction Forces, Journal of Ship Research, 54 (2010) 79-94.

[20] X.S. Zhang, P. Bandyk, R.F. Beck, Seakeeping computations using double-body basis flows, Applied Ocean Research, 32 (2010) 471-482.

[21] Y. Kim, D.K.P. Yue, B.S.H. Connell, Numerical dispersion and damping on steady waves with forward speed, Appl. Ocean Res, 27 (2005) 107-125.

[22] M.S. Longuet-Higgins, E.D. Cokelet, The deformation of steep surface waves on water. I. A numerical method of computation, in: Proceedings of the Royal Society of London A: Mathematical, Physical and Engineering Sciences, The Royal Society, 1976, pp. 1-26.

[23] H. Xu, D. Yue, Computations of fully nonlinear three dimensional water waves, in: Proceedings of the 19th Symposium On Naval Hydrodynamics, Seoul, Korea, 1992.

[24] T.H.J. Bunnik, Seakeeping calculations for ships, taking into account the non-linear steady waves, in, Delft University of Technology, Delft, Netherlands, 1999.

[25] M. Kashiwagi, M. Ohkusu, A new theory for side-wall interference effects on forward-speed radiation and diffraction forces, Ship Technol. Res, 38 (1991) 17-48.

[26] X. Feng, W. Bai, Wave resonances in a narrow gap between two barges using fully nonlinear numerical simulation, Applied Ocean Research, 50 (2015) 119-129.

[27] X. Feng, W. Bai, X.B. Chen, L. Qian, Z.H. Ma, Numerical investigation of viscous effects on the gap resonance between side-by-side barges, Ocean Eng, 145 (2017) 44-58.

[28] W. Zhao, I.A. Milne, M. Efthymiou, H.A. Wolgamot, S. Draper, P.H. Taylor, R.E. Taylor, Current practice and research directions in hydrodynamics for FLNG-side-by-side offloading, Ocean Eng, 158 (2018) 99-110.